JOURNAL OF GUIDANCE, CONTROL, AND DYNAMICS
Vol. 32, No. 1, January–February 2009

Control of Science Orbits About Planetary Satellites

Marci Paskowitz Possner*
GMV Space Systems, Inc., Rockville, Maryland 20850
and
Daniel J. Scheeres†
University of Colorado at Boulder, Boulder, Colorado 80309

DOI: 10.2514/1.36220

In this paper, control issues for science orbits about planetary satellites are investigated. The science orbits have low altitudes, near-polar inclinations, and follow the stable and unstable manifolds of frozen orbits. The effect of orbit uncertainty caused by initial position errors is studied, and criteria are identified to ensure the desired behavior for the orbits. Two schemes to control a planetary satellite orbiter are developed as follows: 1) given the terminal conditions of a science orbit, redesign a new science orbit and execute a low-cost transfer to it, and 2) return the spacecraft to its nominal trajectory via a two-sequence set of maneuvers. In the first scheme, the method used is a two-maneuver transfer that is optimized for the smallest total Δv. The resulting steady-state costs for transfers of orbits about Europa are on the order of 30 cm/s/day, corresponding to two maneuvers of 16 m/s each. For the second scheme, Monte Carlo analysis is used to determine the effect of initial position errors, with results showing that if the initial trajectory is biased correctly, initial position errors do not significantly affect the trajectory. A two-maneuver Hohmann transfer is designed to return the spacecraft to the nominal trajectory if needed, with costs on the order of 1 m/s for Europa.

Introduction

THE exploration of planetary satellites by robotic spacecraft is currently of strong scientific interest. One of the challenges of planning such a mission is the design of the science orbit, which is the orbit where the acquisition of scientific data takes place. Science orbits for missions to planetary satellites have, in general, low altitudes and near-polar inclinations so that the entire surface can be mapped, and the science requirements of the mission can be accomplished. These requirements may include imaging the surface, determining its composition, and measuring features of the planetary satellite such as the gravity field and the radiation environment. However, designing such an orbit can be very difficult because the dynamical environment of many planetary satellites is highly perturbed with respect to an integrable two-body system due to their proximity to their central planet. One such example is Jupiter's moon Europa, which has been the subject of a few proposed missions in recent years.

The analysis of the dynamics governing the motion of a spacecraft in the vicinity of a planetary satellite has been extensively studied. One of the primary methods of this analysis is averaging, a technique which approximates the system by reducing the degrees of freedom, allowing for analytic studies [1–4]. Once the dynamics of such systems are better understood, the design of science orbits is possible. When designing these orbits, the main goal is to find trajectories that have long lifetimes and that satisfy the criteria described above. The long lifetime condition is important, even if the science phase of a mission to a planetary satellite is not going to be very long. This is because it is necessary to ensure that even if a maneuver failure occurs, the spacecraft would not immediately impact with the planetary satellite or leave the region. It is possible to design science orbits using techniques other than averaging such as the computation of periodic orbits, as in [5]. However, for the results in this paper, we build on the results in [6], where long lifetime science orbits are designed using the results from averaging analysis.

There are different ways to approach the problem of the control of science orbits. What would seem to be the simplest is using constant thrust to keep the orbital elements frozen. However, analysis of the cost of using a technique such as this shows that the cost of using a constant thrust is prohibitively large and is not practical for a mission [7]. The types of control thrust evaluated were both thrust in the purely radial direction and thrust in the purely transverse direction and the required costs were found to range from 10 to 100 m/s/day. Thus in this paper we investigate the use of impulsive maneuvers to guide the spacecraft back to a nominal trajectory.

The first technique considered is to allow the orbit to evolve from its initial point at the minimum eccentricity location [7] on the stable manifold to the minimum eccentricity point on the unstable manifold. The minimum eccentricity locations are points on the stable and unstable manifold where the eccentricity reaches a minimum on either side of the frozen orbit. Then, two maneuvers are performed to reset the orbit back to the stable manifold. Instead of requiring that the spacecraft return to the same initial point, some of its current characteristics such as the radius of periapsis and inclination are used to design a new long lifetime orbit. Finally, the two maneuvers are optimized for the lowest cost transfer to the new target. The ideal transfer is a circularization maneuver followed by a maneuver to increase the eccentricity at a location on the transfer orbit that would set the argument of periapsis appropriately. That sequence is used as a starting guess for the optimization routine that optimizes over the total cost of both transfer maneuvers. We find that the cost to do both maneuvers is fairly low (on the order of 30 cm/s/day for Europa) and is practical for a real mission.

The second control issue discussed is correcting the spacecraft's position on the designed long lifetime trajectory if it drifts too far away. Monte Carlo analysis of trajectories with initial errors shows that errors within the range of uncertainty for a mission to Europa [8] can cause the trajectory to follow the wrong manifold path. Because initial errors in the spacecraft's position can destroy the long lifetime properties of the trajectory, it is important to determine ways to get the spacecraft back on the correct orbit with a relatively low cost. We show that if the erroneous trajectory is integrated along with the correct trajectory for several days and then a sequence of maneuvers is designed to place the spacecraft at the correct location

Received 15 December 2007; revision received 5 August 2008; accepted for publication 6 August 2008.

*Lead Flight Dynamics Engineer; mpossner@gmvspacesystems.com. Member AIAA.

†A. Richard Seebass Chair, Colorado Center for Astrodynamics Research; scheeres@colorado.edu. Associate Fellow AIAA.

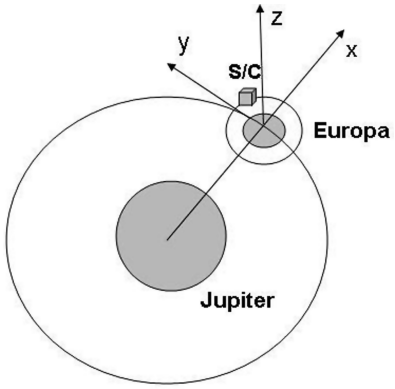

Fig. 1 Geometry of the Europa orbiter model.

corresponding to the time of the correction, the cost of the correction is very low. The transfer is a two-maneuver sequence, optimized for the total cost. The ideal transfer is a Hohmann-type transfer between two elliptic orbits and this is used as the initial guess of the optimization. This technique results in costs of less than 1 m/s (for Europa) for corrections done up to 10 days after the initial time and is a realistic technique for a real mission.

Background

In this section, some background information necessary for the remainder of the results is presented. This information is discussed in detail in [6], and so only a summary is presented here. However, the concepts are key to this paper and thus must be restated.

Definition of the System

The physical situation we consider consists of a spacecraft in orbit about a planetary satellite which is in turn in orbit about a planet (see Fig. 1). In particular, we consider a spacecraft orbiting Jupiter's moon Europa. We include the first-order perturbing effect of the planet's gravity on the planetary satellite, as well as the J_2, C_{22}, and J_3 gravity effects of the planetary satellite. Those three terms from Europa's gravity field are included because they have been found to strongly affect the dynamics being considered in this analysis and the orbit lifetimes. Note that when including C_{22}, we assume that Europa's rotation rate about its maximum moment of inertia is synchronous with its orbit rate and that its axis with the minimum moment of inertia is aligned with the Jupiter–Europa line. The numerical values for the parameters used in this paper are presented in Table 1.

The perturbing potential is the addition of the four contributing perturbations [9,10]:

$$R = \frac{1}{2}N^2(3x^2 - r^2) - \frac{\mu J_2}{2}\left(\frac{3z^2}{r^5} - \frac{1}{r^3}\right) + \frac{3\mu C_{22}}{r^5}(x^2 - y^2) - \frac{\mu J_3}{2}\left(\frac{5z^3}{r^7} - \frac{3z}{r^5}\right) \tag{1}$$

This potential corresponds to a modified form of Hill's three-body problem, incorporating gravity coefficients for the central attracting body. The general equations of motion for a system in this form are

Table 1 Parameters of Europa

Parameter	Symbol	Value
Europa radius	R_E	1560.8 km
Europa orbital period	T	3.55 days
Europa orbit rate	N	2.05×10^{-5} rad/s
Europa gravitational parameter	μ	3.201×10^3 km^3/s^2
Nondimensional Europa J_2 [a]	J_2/R_E^2	4.2749×10^{-4}
Nondimensional Europa C_{22} [a]	C_{22}/R_E^2	1.2847×10^4
Nondimensional Europa J_3 [a]	J_3/R_E^3	1.3784×10^{-4}

[a]Values obtained from John Aiello, personal communication, August 2004.

$$\ddot{x} + 2N\dot{y} = -\frac{\mu}{r^3}x + N^2x + \frac{\partial R}{\partial x} \tag{2}$$

$$\ddot{y} - 2N\dot{x} = -\frac{\mu}{r^3}y + N^2y + \frac{\partial R}{\partial y} \tag{3}$$

$$\ddot{z} = -\frac{\mu}{r^3}z + \frac{\partial R}{\partial z} \tag{4}$$

where x is measured along the line from the planet to the planetary satellite, r is the orbital radius from the center of the planetary satellite, and N and μ are the orbit angular rate and gravitational parameter, respectively, of the planetary satellite. Equations (2–4) with the potential in Eq. (1) are referred to as the 3-DOF (degree of freedom) system.

Science Orbit Design

The design of science orbits about planetary satellites begins with the analysis of the unstable near-circular, near-polar frozen orbits that exist in the 1-DOF system. The 1-DOF system is computed by averaging the 3-DOF system over the orbit of the spacecraft around the planetary satellite and over the orbit of the planetary satellite about the planet. The resulting 1-DOF potential is [6]

$$\tilde{R} = \frac{N^2a^2}{4}\left[\left(1 - \frac{3}{2}\sin^2 i\right)\left(1 + \frac{3}{2}e^2\right) + \frac{15}{4}e^2\cos 2\omega\sin^2 i\right] + \frac{\mu J_2}{2a^3(1-e^2)^{3/2}}\left(1 - \frac{3}{2}\sin^2 i\right) + \frac{3\mu J_3}{2a^4(1-e^2)^{5/2}}e\sin\omega\sin i\left(1 - \frac{5}{4}\sin^2 i\right) \tag{5}$$

Note that the C_{22} component vanishes under the averaging. The frozen orbits are the equilibrium solutions to the following Lagrange planetary equations [11], computed using the 1-DOF potential:

$$\frac{de}{dt} = \frac{15}{8}\frac{N^2}{n}e\sqrt{1-e^2}\sin^2 i\sin 2\omega - \frac{3J_3 n}{2a^3(1-e^2)^3}\sin i\left(1 - \frac{5}{4}\sin^2 i\right)\cos\omega \tag{6}$$

$$\frac{di}{dt} = -\frac{15}{16}\frac{N^2}{n}\frac{e^2}{\sqrt{1-e^2}}\sin 2i\sin 2\omega + \frac{3nJ_3}{2a^3(1-e^2)^3}e\cos i\left(1 - \frac{5}{4}\sin^2 i\right)\cos\omega \tag{7}$$

$$\frac{d\omega}{dt} = \frac{3}{8}\frac{N^2}{n}\frac{1}{\sqrt{1-e^2}}[5\cos^2 i - 1 + 5\sin^2 i\cos 2\omega + e^2(1 - 5\cos 2\omega)] + \frac{3nJ_2}{4a^2(1-e^2)^2}\left(1 - \frac{5}{4}\sin^2 i\right) + \frac{3J_3 n}{2a^3(1-e^2)^3}\frac{\sin\omega\sin i}{e}\left[\left(1 - \frac{5}{4}\sin^2 i\right)(1 + 4e^2) - \frac{e^2}{\sin^2 i}\left(1 - \frac{19}{4}\sin^2 i + \frac{15}{4}\sin^4 i\right)\right] \tag{8}$$

The frozen orbits considered in this analysis are those that are the most suitable for the development of long lifetime science orbits, with near-polar inclinations, near-circular eccentricities, and $\omega = \pi/2$ [6]. These frozen orbits are unstable, meaning that although they cannot be used directly as long lifetime science orbits, they can be used as a first step toward computing them.

Because the 1-DOF system is Hamiltonian, the frozen orbits have stable and unstable manifolds. If a spacecraft is initialized on the stable manifold of a frozen orbit, it will drift toward the frozen orbit

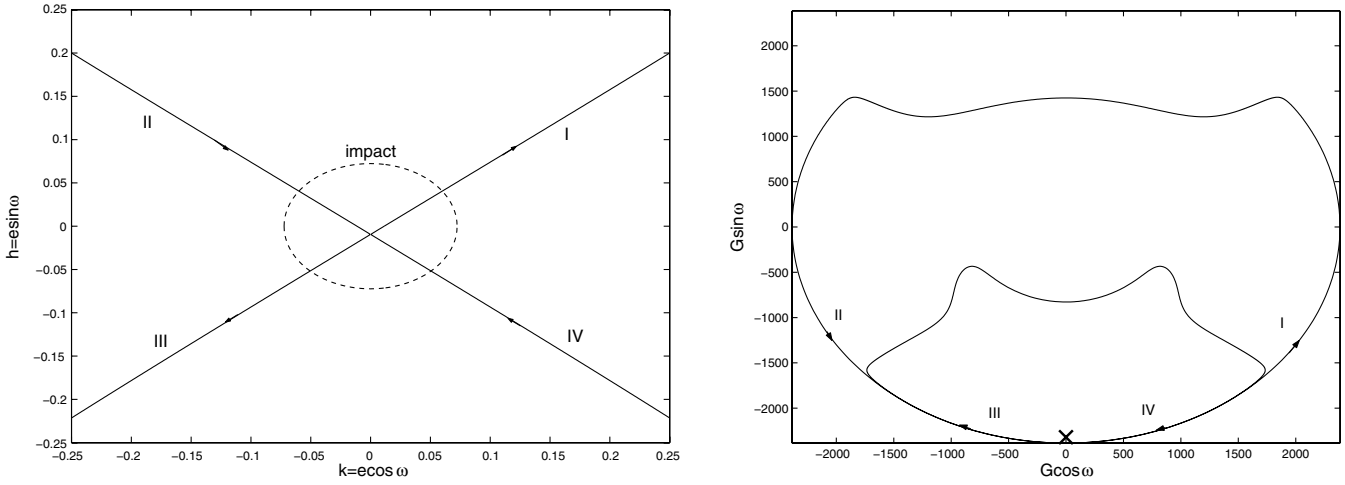

a) (*h*,*k*) space **b) (*G*,*ω*) space**

Fig. 2 Stable and unstable manifolds for a frozen orbit, identified with an ×, with $e^* = 0.0129$, $i^* = 70$ deg, $\omega^* = -90$ deg, and $a^* = 1682.5$ km.

location on the stable manifold, and then follow the unstable manifold toward impact with the planetary satellite. The manifolds of the frozen orbits are determined by computing the contour of constant potential $\tilde{R}$ [6] that passes through the frozen orbit. The manifolds are plotted in the two different regimes, (h, k) and (G, ω), where $h = e\sin\omega$, $k = e\cos\omega$, and $G = \sqrt{\mu a(1-e^2)}$ [10]. Figure 2 shows the stable and unstable manifolds for a frozen orbit with a 70 deg inclination, with the unstable manifolds numbered I and III and the stable manifolds numbered II and IV. From Fig. 2b, the number of degrees of ω covered along each of the four paths while the trajectory is near circular can be determined. Once the trajectory departs from its near-circular value, the radius of periapsis will decrease to below the surface of the planetary satellite because the semimajor axis remains constant (in Fig. 2b, this is where the contour moves inward). The impact circle is shown in Fig. 2a. The four possible paths and approximate number of degrees of ω covered along each path are as follows: 1) II $\rightarrow$ I: 270 deg, 2) II $\rightarrow$ III: 180 deg, 3) IV $\rightarrow$ I: 180 deg, and 4) IV $\rightarrow$ III: 90 deg.

Different ranges of ω are covered along different paths because the frozen orbits are not circular. The path that produces the longest lifetime trajectory is the II $\rightarrow$ I path because the most degrees of ω are covered while the orbit is near circular.

In the 3-DOF system, the trajectory will not follow the manifolds exactly. It is possible, however, to determine initial conditions such that this path along the manifold is followed on average and very long lifetime orbits are attained. The procedure to compute the initial conditions for long lifetime science orbits is summarized in Table 2 and described in detail in [6]. Note that the minimum eccentricity point on the stable manifold is the point where the eccentricity reaches a minimum before increasing to the frozen orbit eccentricity. It has advantages that are exploited in the orbit control analysis. Details on how it is computed can be found in [7].

The numerical search over the argument of periapsis values (step 5 in Table 2), called a bias, is sometimes necessary to produce an orbit that follows the II $\rightarrow$ I manifold path. The correction is needed because the initial conditions computed up to step 4 use a linearization which only approximates the 3-DOF motion. The method used to compute the bias is a numerical search. It begins with a search using a coarse step size through argument of periapsis values in the vicinity of the initial value (computed in step 4 of Table 2). The search region is then successively narrowed around the maximum with decreasing step sizes until the maximum lifetime orbit is found, to an accuracy of 0.0002 rad. We define a general long lifetime science orbit as a trajectory that follows the correct (II $\rightarrow$ I) manifold path. The trajectory that has the manifold as its exact average (the frozen orbit contour) is called the maximum lifetime orbit. However, as will be shown later, this trajectory is generally not practical as a science orbit for a real mission. Table 3 gives the lifetimes for a few general and maximum lifetime orbits.

Resetting a Long Lifetime Science Orbit

Although the orbits described in the previous section have long lifetimes, they are finite and the spacecraft will eventually follow the unstable manifold to impact with the planetary satellite. It is important to develop a control strategy to delay impact with the

Table 2 Algorithm for computing a long lifetime orbit

1	Choose frozen orbit in the 1-DOF system based on its inclination.
2	Compute the minimum eccentricity point on the stable manifold of the frozen orbit.
3	Compute the corrected initial conditions to the 2-DOF system by using the linearization of the 2-DOF system about the point on the manifold.
4	Compute the corrected initial conditions to the 3-DOF system by using the linearization of the 3-DOF system about the corrected 2-DOF initial conditions.
5	Find an argument of periapsis value that produces a long lifetime orbit by numerical search, if necessary.

Table 3 Long lifetime orbits for the Europa system

Frozen orbit inclination	Unbiased lifetime, days	Maximum lifetime, days	Bias, rad
70 deg	105	182	0.0095
75 deg	119	174	0.0026
85 deg	110	171	0.0046
95 deg	96	182	0.0169
105 deg	95	172	0.0254
110 deg	99	188	0.0242

planetary satellite. Because an algorithm to design long lifetime orbits already exists, it is natural to use this algorithm during the development of the control scheme. The technique used to control the long lifetime orbit is to allow the trajectory to reach the unstable manifold and then, at a certain point, reset it back to the stable manifold so another long lifetime orbit can evolve.

Designing the Target

The initial conditions of a long lifetime orbit are computed by starting at the minimum eccentricity point on the manifold and are a specific 6-state. The minimum eccentricity point on the manifold corresponds to a particular frozen orbit which in turn corresponds to a specific radius of periapsis. As the orbit evolves, the orbital elements oscillate, and in particular, the radius of periapsis oscillates. Therefore, when the orbit is stopped on the unstable manifold, resetting it back to the original long lifetime orbit initial conditions is very difficult because the modification of all of the parameters of the orbit would be necessary. Because the goal is simply to prevent the impact of the spacecraft with the planetary satellite by resetting the trajectory to the stable manifold, it is not necessary to reset it to the same long lifetime orbit. Therefore, at the point that the orbit is stopped on the unstable manifold a new long lifetime orbit is computed, with parameters consistent with the current orbital parameters.

Denote the initial conditions of the new long lifetime orbit to be designed by the target. The first step in designing the target is to specify its corresponding frozen orbit. Because the algorithm used to design long lifetime orbits places the spacecraft at the minimum eccentricity point on the stable manifold, it is logical to stop the orbit at the minimum eccentricity point on the unstable manifold. This minimizes the eccentricity changes that will be required during the transfer. For simplicity in the design, the stopping point used is actually the first periapsis passage after the minimum eccentricity point on the unstable manifold. In the ideal 1-DOF system, there are no oscillations while the trajectory moves from its initial point on the stable manifold to the stopping point on the unstable manifold. Thus, to reset the orbit to the stable manifold, only the argument of periapsis needs to be changed. The easiest way to do this is a two-maneuver sequence consisting of a circularization at the stopping point and a maneuver to increase the eccentricity at $\omega + \nu = \omega_{ll}$, where ω_{ll} is the initial argument of periapsis of the original long lifetime orbit. Because the ideal transfer orbit is circular, this resets the orbit to its original point on the stable manifold. See Fig. 3 for a diagram of this reset scheme in the 1-DOF system. Obviously this system is not the ideal 1-DOF system and there are perturbations present. However, the ideal transfer can be used to generate a target in the 3-DOF system.

The first step is to circularize the orbit at the stopping point and let the orbit evolve in the 3-DOF system until $\omega + \nu = \omega_{ll}$. Denote this point with the subscript "IT" (ideal target). Then, the frozen orbit to be used in the actual target design has a radius of periapsis equal to r_{IT} and an inclination equal to i_{IT}. The frozen orbit eccentricity can then be computed along with the minimum eccentricity on the new manifold. Using all of these values, the initial conditions of a new long lifetime orbit can be computed using the algorithm in Table 2. Note that $\tilde{\Omega}_{\mathrm{IT}} = \Omega_{\mathrm{IT}} - N t_{\mathrm{IT}}$. Because the target is always designed for time equal to zero, $\tilde{\Omega}_0 = \Omega_{\mathrm{IT}}$. The orbital elements of the target are denoted with the subscript T. A summary of the procedure for computing the target is as follows:

1) Stop the original long lifetime trajectory at the first periapsis after the minimum eccentricity point on the unstable manifold.

2) Perform the "ideal transfer" which consists of a circularization at the stopping point and integrate until $\omega + \nu = \omega_{\mathrm{original}}$.

3) Let the frozen orbit corresponding to the target have a radius of periapsis and inclination of r_{IT} and i_{IT}, respectively, and $\tilde{\Omega}_0 = \Omega_{\mathrm{IT}}$.

4) Compute the target position using the algorithm for computing long lifetime orbits in Table 2.

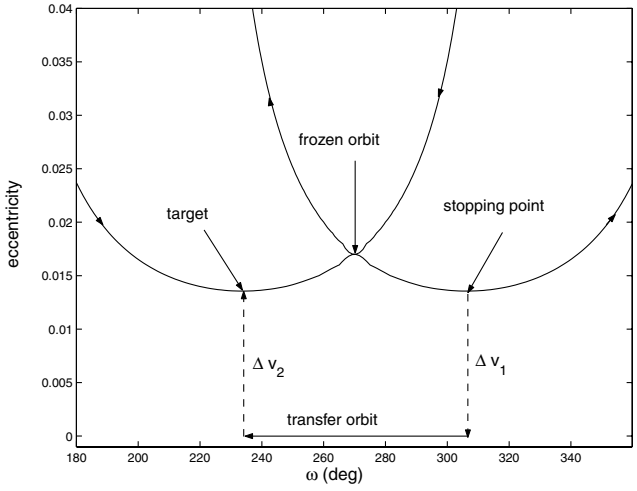

Fig. 3 Diagram of the reset scheme in the 1-DOF system in (e,ω) space.

Transferring to the Target

The next step is determining how to transfer to the target, knowing that there are perturbations present which prevent the use of the ideal transfer described previously. Note, however, that the ideal transfer is a good first estimate. Therefore, we start with the circularization burn and integrate until $\omega + \nu = \omega_T$. Denote the transfer time t_f. Aside from reaching the target, our goal is also to minimize the total cost of the transfer, which consists of two burns—one at periapsis on the unstable manifold and one at the target. First, we focus on reaching the target. Let $\mathbf{r}_T$ denote the target position and $\mathbf{v}_T$ the target velocity. Then,

$$\mathbf{r}_T = \mathbf{r}(t_f, \mathbf{r}_0, \mathbf{v}_0 + \delta\mathbf{v}) \tag{9}$$

$$\mathbf{v}_T = \mathbf{v}(t_f, \mathbf{r}_0, \mathbf{v}_0 + \delta\mathbf{v}) \tag{10}$$

where $\mathbf{r}_0$ and $\mathbf{v}_0$ correspond to the stopping point (at periapsis) on the unstable manifold and $\delta\mathbf{v}$ is the first burn. A Taylor expansion of Eq. (9) yields

$$\mathbf{r}_T = \mathbf{r}(t_f) + \left.\frac{\partial \mathbf{r}}{\partial \mathbf{v}_0}\right|_{t_f} \delta\mathbf{v} + \cdots \tag{11}$$

Then, keeping only first-order terms and rearranging for $\delta\mathbf{v}$:

$$\delta\mathbf{v} = \left(\frac{\partial \mathbf{r}}{\partial \mathbf{v}_0}\right)^{-1}\Bigg|_{t_f} (\mathbf{r}_T - \mathbf{r}_0) \tag{12}$$

Denote the state transition matrix as

$$\Phi(0, t_f) = \begin{pmatrix} \phi_{rr} & \phi_{rv} \\ \phi_{vr} & \phi_{vv} \end{pmatrix} \tag{13}$$

Then,

$$\left.\frac{\partial \mathbf{r}}{\partial \mathbf{v}_0}\right|_{t_f} = \phi_{rv}$$

Also, let $\delta\mathbf{r} = (\mathbf{r}_T - \mathbf{r}(t_f))$. We can converge on the $\delta\mathbf{v}$ necessary for the transfer orbit to end at the target $\mathbf{r}_T$ using the following iteration until $\delta\mathbf{r} = 0$:

$$\delta\mathbf{v} = \delta\mathbf{v}_0 + \delta\mathbf{v}_1 + \delta\mathbf{v}_2 + \cdots \tag{14}$$

where

$$\delta\mathbf{v}_{i+1} = \phi_{rv}^{-1}\delta\mathbf{r}_i \tag{15}$$

The above method ensures that the spacecraft reaches the target position by the end of the transfer orbit. At the target position a second burn is executed such that the spacecraft velocity is equal to the target velocity. The first burn is $\delta\mathbf{v}$ and the second burn is

$\mathbf{v}_T - \mathbf{v}(t_f)$. However, this method does not optimize the total cost. Therefore, the next step is refining the transfer orbit and hence the maneuvers to reduce the cost of both burns. Let $\Delta\mathbf{v}_1^* = \delta\mathbf{v}$ and $\Delta\mathbf{v}_2^* = \mathbf{v}_T - \mathbf{v}(t_f)$. Then, consider a correction to the transfer time t_f, denoted as δt, needed to optimize the total cost. This necessitates the introduction of corrections to both burns $\delta\mathbf{v}_1$ and $\delta\mathbf{v}_2$. The target position and velocity are now

$$\mathbf{r}_T = \mathbf{r}(t_f + \delta t, \mathbf{r}_0, \mathbf{v}_0 + \Delta\mathbf{v}_1^* + \delta\mathbf{v}_1) \tag{16}$$

$$\mathbf{v}_T = \mathbf{v}(t_f + \delta t, \mathbf{r}_0, \mathbf{v}_0 + \Delta\mathbf{v}_1^* + \delta\mathbf{v}_1) + \Delta\mathbf{v}_2^* + \delta\mathbf{v}_2 \tag{17}$$

A Taylor series expansion of Eqs. (16) and (17) yields

$$\mathbf{r}_T = \mathbf{r}(t_f) + \left.\frac{\partial\mathbf{r}}{\partial t}\right|_{t_f}\delta t + \left.\frac{\partial\mathbf{r}}{\partial\mathbf{v}_0}\right|_{t_f}\delta\mathbf{v}_1 + \cdots \tag{18}$$

$$\mathbf{v}_T = \mathbf{v}(t_f) + \left.\frac{\partial\mathbf{v}}{\partial t}\right|_{t_f}\delta t + \left.\frac{\partial\mathbf{v}}{\partial\mathbf{v}_0}\right|_{t_f}\delta\mathbf{v}_1 + \cdots + \Delta\mathbf{v}_2^* + \delta\mathbf{v}_2 \tag{19}$$

Then, truncating at first order in the Taylor expansions and noting that $\mathbf{r}_T = \mathbf{r}(t_f)$ and $\mathbf{v}_T = \mathbf{v}(t_f) + \Delta\mathbf{v}_2^*$, we obtain the following expressions for $\delta\mathbf{v}_1$ and $\delta\mathbf{v}_2$:

$$\delta\mathbf{v}_1 = -\left(\frac{\partial\mathbf{r}}{\partial\mathbf{v}_0}\right)^{-1}\Bigg|_{t_f}\mathbf{v}(t_f)\delta t \tag{20}$$

$$\delta\mathbf{v}_2 = -\left(\left.\frac{\partial\mathbf{v}}{\partial t}\right|_{t_f} + \left.\frac{\partial\mathbf{v}}{\partial\mathbf{v}_0}\right|_{t_f}\delta\mathbf{v}_1\right)\delta t \tag{21}$$

Using the definition of the state transition in Eq. (13),

$$\phi_{rv} = \left.\frac{\partial\mathbf{r}}{\partial\mathbf{v}_0}\right|_{t_f}$$

and

$$\phi_{vv} = \left.\frac{\partial\mathbf{v}}{\partial\mathbf{v}_0}\right|_{t_f}$$

The expressions for $\delta\mathbf{v}_1$ and $\delta\mathbf{v}_2$ are then

$$\delta\mathbf{v}_1 = -\phi_{rv}^{-1}\mathbf{v}(t_f)\delta t \tag{22}$$

$$\delta\mathbf{v}_2 = -[\mathbf{a}(t_f) - \phi_{vv}\phi_{rv}^{-1}\mathbf{v}(t_f)]\delta t \tag{23}$$

where $\mathbf{a}(t_f)$ is the acceleration at t_f.

The goal of this scheme is to minimize the total cost. Let the cost function be

$$J = (\Delta\mathbf{v}_1^* + \delta\mathbf{v}_1)^2 + (\Delta\mathbf{v}_2^* + \delta\mathbf{v}_2)^2 \tag{24}$$

Since $\delta\mathbf{v}_1$ and $\delta\mathbf{v}_2$ are functions of δt, denote them as $\delta\mathbf{v}_1 = \alpha_1\delta t$ and $\delta\mathbf{v}_2 = \alpha_2\delta t$. Then, J can be expressed as

$$J = |\Delta\mathbf{v}_1^*|^2 + |\Delta\mathbf{v}_2^*|^2 + 2[(\Delta\mathbf{v}_1^*)^T\alpha_1 + (\Delta\mathbf{v}_2^*)^T\alpha_2]\delta t + (|\alpha_1|^2 + |\alpha_2|^2)\delta t^2 \tag{25}$$

$$= A\delta t^2 + 2B\delta t + C \tag{26}$$

Because the cost J is a function of δt, take the derivative of J with respect to δt and set it equal to zero to minimize the cost:

$$\frac{\partial J}{\partial\delta t} = 2A\delta t + 2B = 0 \tag{27}$$

Therefore, the δt required to minimize the total cost is

$$\delta t = -\frac{B}{A} \tag{28}$$

where

$$A = \mathbf{v}(t_f)^T\phi_{rv}^{-T}\phi_{rv}^{-1}\mathbf{v}(t_f) + [\mathbf{a}(t_f) - \phi_{vv}\phi_{rv}^{-1}\mathbf{v}(t_f)]^T[\mathbf{a}(t_f) - \phi_{vv}\phi_{rv}^{-1}\mathbf{v}(t_f)] \tag{29}$$

$$B = -(\Delta\mathbf{v}_1^*)^{-1}\phi_{rv}^{-1}\mathbf{v}(t_f) - (\Delta\mathbf{v}_2^*)^T[\mathbf{a}(t_f) - \phi_{vv}\phi_{rv}^{-1}\mathbf{v}(t_f)] \tag{30}$$

The overall procedure to compute the maneuvers necessary to transfer the spacecraft from a periapsis location on the unstable manifold to a new long lifetime orbit initialized on its stable manifold is as follows:

1) Compute the ideal transfer consisting of a circularization at periapsis on the unstable manifold and an integration until $\omega + \nu = \omega_T$. Let the time required for this transfer be t_f.

2) Use the iteration scheme

$$\delta\mathbf{v} = \delta\mathbf{v}^0 + \delta\mathbf{v}^1 + \delta\mathbf{v}^2 + \cdots \tag{31}$$

where

$$\delta\mathbf{v}^{i+1} = \phi_{rv}^{-1}\delta\mathbf{r}_i \tag{32}$$

to compute the necessary correction to the first burn such that $\delta\mathbf{r} = 0$.

3) Let $\Delta\mathbf{v}_1^* = \delta\mathbf{v}$ and $\Delta\mathbf{v}_2^* = \mathbf{v}_T - \mathbf{v}(t_f)$ and compute new corrections to the burns, $\delta\mathbf{v}_1$ and $\delta\mathbf{v}_2$, to minimize the cost using $\delta t = -\frac{B}{A}$.

4) Repeat steps 2 and 3 until $\delta t_{i+1} - \delta t_i < 10^{-9}$.

The optimization scheme described above does not actually minimize the total cost, but minimizes the sum of the squares of the two burns. To minimize the total cost would require $J = |\Delta\mathbf{v}_1^* + \delta\mathbf{v}_1| + |\Delta\mathbf{v}_2^* + \delta\mathbf{v}_2|$. However, testing of both methods results in approximately the same total cost for both cases and so the sum of the squares method is used because it is computationally simpler.

Examples

The examples detailed in this section show that the technique described above provides a practical way to reset a long lifetime orbit with a relatively low cost. As previously mentioned, it is not necessary to find the maximum lifetime orbit on a particular manifold because it would not be achievable in a real mission. However, it is important to ensure that the long lifetime orbit follows the correct manifold. The long lifetime orbits used in these examples are those in Table 3 (the unbiased long lifetime orbits, not the maxima). These unbiased long lifetime orbits all follow the correct manifold path. However, when the target long lifetime orbit is computed, we must verify that it too follows the correct long lifetime path. We found that of the six examples computed, the 85 and 95 deg orbits follow the correct manifold path and the others do not. For the four that do not follow the correct manifold path, a bias in the argument of periapsis is included. This bias does not correspond to the longest lifetime orbit, but to a long lifetime orbit that follows the correct manifold path and has a lifetime in the 100–110 day vicinity. This range was chosen so that all of the target orbits have approximately the same lifetimes. This eases the comparison of the costs associated with the transfers.

Table 4 shows the details of the examples, identified by the inclination of the associated frozen orbit of the original long lifetime trajectory. For each orbit, the magnitude of each of the two burns, the lifetime of the target trajectory, and the bias used for the target trajectory (if necessary) are given. The point of comparison for each example is the average cost per day. This is computed by dividing the total cost of the two maneuvers by the lifetime of the target trajectory. It is clear that this method has a much lower cost than both the radial and transverse low-thrust methods. Specifically, the average cost per day here is an order of magnitude less than the transverse thrust law and 2 orders of magnitude less than the radial thrust law. Figure 4

Table 4 Examples of long lifetime science orbit reset

Frozen orbit inclination	Δv_1, m/s	Δv_2, m/s	Target trajectory lifetime, days	Target trajectory bias, rad	Cost/day, cm/s
70 deg	16.30	17.94	110	0.06	31.1
75 deg	19.07	21.33	106	0.06	38.1
85 deg	11.20	15.67	99	——	27.1
95 deg	15.45	19.76	103	——	34.2
105 deg	12.32	16.19	106	−0.04	26.9
110 deg	14.36	18.62	107	−0.095	30.8

shows the 1-DOF manifold of an original long lifetime trajectory, the integration of an original long lifetime trajectory, and the integration of a target trajectory. Observe that the target trajectory and original trajectory are very close to each other. Figure 5 shows the time histories of the orbital elements for the original long lifetime trajectory and the target trajectory. Observe that the orbital elements of both trajectories are very close to each other. This is important because resetting the orbit is only useful if the extension of the orbit still satisfies the science requirement of the mission, which it should if this scheme is used.

Orbit Uncertainty

Up to this point, we have assumed that it is possible to attain the desired long lifetime orbits. However, in a real mission, it is important to take the uncertainty of the orbiter's position and velocity into account. In [8], Thompson et al studied orbit determination for a 30-day mission to Europa. They performed simulations using a science orbit with similar characteristics to our long lifetime orbits. In particular, their orbit is near polar, near circular, and has an average 100 km altitude. One of the biggest drivers of the uncertainty of orbits about Europa is the lack of knowledge of the Europa gravity field. Only some of the second degree terms of the Europa gravity field are currently known, and they were determined from Galileo flybys of Europa [12].

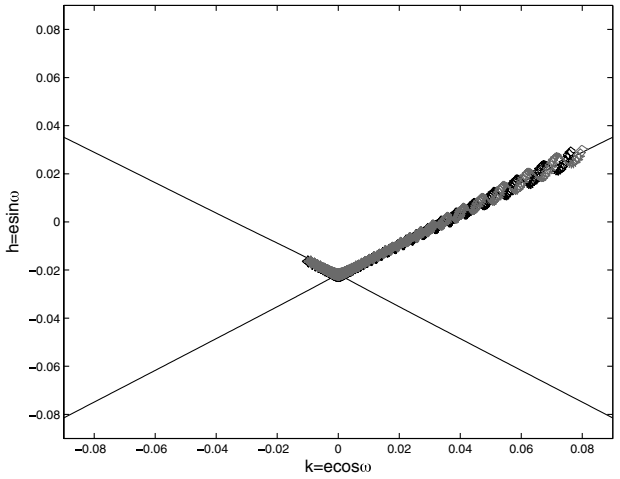

Fig. 4 Original (black) and target (gray) long lifetime trajectories.

The first study performed in [8] uses a worst-case gravity error, which assumes that no additional knowledge of Europa's gravity field is known during the science phase of the mission. This results in errors in the spacecraft's radial, cross-track, and along-track position components on the order of kilometers. These results agree with those in [13]. These errors are judged to be unacceptable for a Europa orbiter mission, and so a further assumption is made. It is assumed that before the science orbit phase of the mission, two weeks of tracking data during orbit conditions similar to the science orbit are available. These data reduce the error in the gravity field. The best-case scenario, which is a lower bound on the gravity error, is computed to provide a gravity field estimate up to degree 20. This results in predicted position errors of 5.1, 7.3, and 5.7 m (3-σ) for radial, cross-track, and along-track position components, respectively. The radial component points from the planetary satellite to the spacecraft, the along-track component points in the direction of the velocity, and the cross-track component completes the triad. However, they assume that a more realistic assumption for the gravity error is in between the best-case and the worst-case (lower and upper) bounds. Using this gravity error results in predicted position errors 24 h after a data cutoff of 48, 60, and 35 m for radial, cross-track and along-track positions, respectively, (also 3-σ values).

Using the results in [8] as a guide, we study how errors in the spacecraft's position affect the designed long lifetime orbits. To study the orbit uncertainty of long lifetime orbits, Monte Carlo simulations are performed. A large number of trajectories are integrated, each with a random initial position error. The initial position error is randomly determining for radial, cross-track, and along-track errors using a Gaussian distribution with a particular standard deviation. The first set of results are for 3-σ values

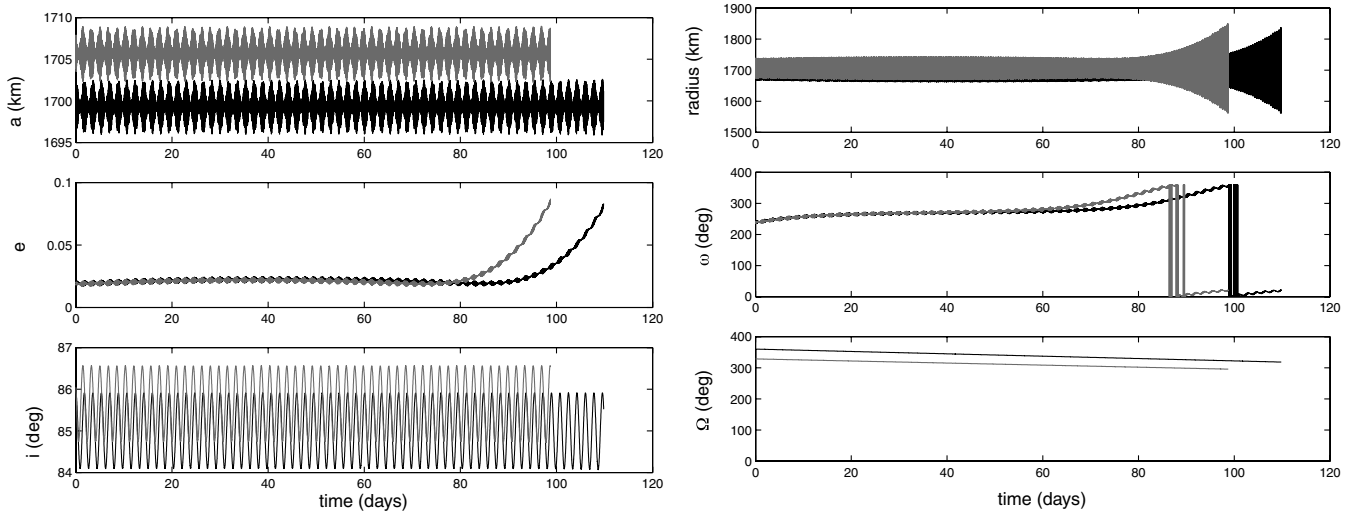

Fig. 5 Time histories of the orbital elements of the original (black) and target (gray) long lifetime trajectories.

Table 5 Monte Carlo results for long lifetime orbits

	Original orbit		Maximum orbit	
Frozen orbit inclination	Lifetime	Correct %	Lifetime	Correct %
70 deg	105 days	100.0	182 days	47.2
75 deg	119 days	78.0	174 days	50.5
85 deg	110 days	92.5	171 days	52.5
95 deg	96 days	100.0	182 days	56.5
105 deg	95 days	100.0	172 days	51.0
110 deg	99 days	100.0	188 days	48.0

corresponding to the realistic gravity error noted previously. Each of the six long lifetime orbits with different inclinations that were previously discussed are considered, with 200 trajectories integrated for each. Recall that the six long lifetime orbits are initialized at the minimum eccentricity point and follow the correct unstable manifold but are not the maximum lifetime orbits for each case.

Table 5 (original orbit column) details the results for all six cases. The lifetime of the nominal orbit is given, along with the percentage of trajectories from the Monte Carlo simulation that follow the correct manifold path. Recall that the correct manifold path is II $\rightarrow$ I path (Fig. 2a). Observe that in four of the six cases, all of the 200 trajectories follow the correct manifold path. For the 75-deg inclination case, 44 of 200 trajectories (22%) follow the wrong manifold path and for the 85-deg inclination case, 15 of 200 trajectories (7.5%) follow the wrong manifold path. These results are explained by taking into account the lifetimes of the six original long lifetime trajectories (Table 2). The two trajectories with the longest lifetimes are the 75 and 85-deg inclination cases. Graphical analysis of the numerical results has shown that a longer lifetime means that the trajectory follows the 1-DOF manifold more closely. The shorter lifetimes that follow the correct manifold path therefore correspond with the trajectories that lie slightly above the manifold. Then, the more closely the correct manifold path is followed, the more likely it is that an initial position error will cause the trajectory to follow the wrong manifold path. Because the 75 and 85-deg inclination orbits have the longest lifetimes, they follow the 1-DOF manifold more closely and therefore it is not surprising that in some cases an initial position error results in a trajectory that follows the wrong manifold path. Further, note that the 75-deg inclination orbit has a longer lifetime than the 85-deg inclination orbit. It follows then that a larger percentage of the trajectories in the 75 deg case follow the wrong path than in the 85 deg case.

The theory that the closer a long lifetime trajectory is to the 1-DOF manifold, the more susceptible it is to errors in the initial position can be further verified by performing Monte Carlo analysis of some maximum long lifetime trajectories. The same maximum lifetime trajectories as those in Table 3 are used, and 200 Monte Carlo simulations are run for each case. The initial position errors are once again determined randomly via a Gaussian distribution with the same 3-σ values as previously. Table 5 shows the results, along with the lifetimes of the maximum lifetime orbits. Observe that the number of trajectories that follow the correct manifold is approximately 50% in each case. This is exactly what is expected because the maximum lifetime trajectories follow the 1-DOF manifolds very closely. Therefore, a small initial position error can bump the trajectory either just above the manifold or just below the manifold. If it is just above the manifold, it will follow the correct manifold path and if it is just below the manifold, it will follow the incorrect manifold path.

It is important when planning a mission to a planetary satellite such as Europa to ensure that the uncertainty error in the position of the spacecraft will not lead to impact with the planetary satellite. Therefore, using the maximum lifetime orbit as the nominal science orbit is not the best course of action because there is about a 50% chance that the spacecraft will deviate too far from the nominal trajectory. The results have shown that the farther above the manifold the long lifetime trajectory is, the more likely it is to follow the correct manifold path. However, the farther above the manifold the trajectory is, the shorter lifetime it has. Choosing the nominal trajectory is therefore a tradeoff between guaranteeing that it will follow the correct manifold path and having a long lifetime. In addition, before the mission starts, the orbit accuracy possible will not be known exactly. The values used here are based on the assumption that before the science portion of the mission the gravity field will be determined with some level of certainty. Even if a trajectory is chosen such that it will always follow the correct manifold path for the error levels used here, it is not certain that this level of orbit accuracy is attainable. Therefore, in the next section we discuss how to return the spacecraft to its nominal orbit once it has drifted away due to an initial error.

Science Orbits with Initial Errors

It is inevitable that during the science phase of a mission to a planetary satellite that the spacecraft will drift away from the nominal trajectory. This will most likely be due to initial errors in the spacecraft's position and velocity. Once it is determined that the spacecraft is no longer on the nominal trajectory, it is important to devise a method for returning it to the nominal trajectory so that the mission can proceed as planned. As shown in the previous section, due to initial position errors, it is possible that a long lifetime trajectory will follow the wrong manifold path. If it does so, it is not possible to use the algorithm to reset the trajectory. Therefore, it is important to return the spacecraft to its nominal trajectory before it has the opportunity to follow the wrong manifold path.

Design of the Correction Maneuvers

The original long lifetime orbit under consideration is determined as usual from the minimum eccentricity point. Initial errors are introduced by randomly determining position errors as in the previous section. A time (in days) is chosen to represent the amount of time until the correction to the trajectory will be made. The amount of time T_E is long enough for the spacecraft to drift away from the nominal trajectory. The maneuvers to be used for the correction are two burns corresponding to a Hohmann-type transfer. Therefore, the initial transfer point should be at periapsis and the target at apoapsis. The initial transfer point is determined by integrating the erroneous trajectory until the closest periapsis passage to T_E (either before or after). Its initial position and velocity are denoted as $\mathbf{r}_0$ and $\mathbf{v}_0$, respectively. In addition, denote its initial longitude of the ascending node as Ω_0.

The nominal trajectory is the long lifetime orbit with no initial errors. The goal of this correction scheme is to transfer the spacecraft to the nominal trajectory. The difficulty lies in determining how to designate the target on the nominal trajectory. Unfortunately, it is not as simple as integrating the nominal trajectory for the same amount of time as the erroneous trajectory and setting the target accordingly. Using this method creates inconsistencies between the initial and target longitude of ascending node values which creates difficulties in converging to the transfer orbit. The method that produces the best results is to integrate the nominal trajectory until its longitude of ascending node value is equal to Ω_0 and then finding the closest periapsis passage to that point (before or after). This periapsis passage on the nominal trajectory therefore corresponds to a point where the spacecraft on the erroneous trajectory should be. Then, the target is set to be the first apoapsis passage following that periapsis passage on the nominal trajectory. Denote the target position and velocity as $\mathbf{r}_T$ and $\mathbf{v}_T$, respectively.

The goal of the transfer is to reach the target and minimize the sum of the squares of the costs of the two burns [Eq. (24)]. The exact same algorithm is used, with the only change being the ideal, first guess transfer orbit. The first guess for the first maneuver is an eccentricity change at periapsis such that the transfer orbit arrives at the target at periapsis. Because, as before, there are perturbations in the system that prevent the target from being reached by this simple method, it is used as a first guess and corrections are made. Figure 6 is a diagram of a Hohmann transfer between two elliptic orbits. Let the semimajor axis of the transfer orbit a_{tr} be given by

$$a_{\text{tr}} = \frac{r_0 + r_t}{2} \tag{33}$$

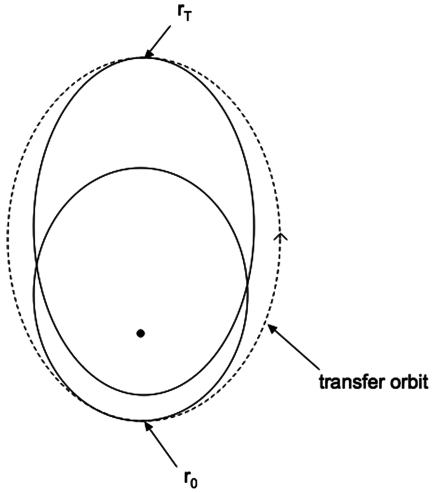

Fig. 6 Schematic of Hohmann transfer between two elliptic orbits.

Then, the velocity of the first guess transfer orbit is

$$\mathbf{v}_g = \sqrt{\mu\left(\frac{2}{r_0} - \frac{1}{a_{\text{tr}}}\right)}\hat{\mathbf{v}}_0 \tag{34}$$

where $\hat{\mathbf{v}}_0$ is the direction of the initial velocity $\mathbf{v}_0$.

The overall procedure to compute the maneuvers necessary to return the spacecraft to its nominal trajectory mirrors the procedure to reset a long lifetime science orbit and is as follows:

1) Compute the ideal transfer consisting of an eccentricity change at periapsis where the velocity is $\mathbf{v}_g$ and integrate to apoapsis. Let the time required for this transfer be t_f.

2) Use the iteration scheme

$$\delta\mathbf{v} = \delta\mathbf{v}^0 + \delta\mathbf{v}^1 + \delta\mathbf{v}^2 + \cdots \tag{35}$$

where

$$\delta\mathbf{v}^{i+1} = \phi_{rv}^{-1}\delta\mathbf{r}_i \tag{36}$$

to compute the necessary correction to the first burn such that $\delta\mathbf{r} = 0$.

3) Let $\Delta\mathbf{v}_1^* = \delta\mathbf{v}$ and $\Delta\mathbf{v}_2^* = \mathbf{v}_t - \mathbf{v}(t_f)$ and compute new corrections to the burns, $\delta\mathbf{v}_1$ [Eq. (22)] and $\delta\mathbf{v}_2$ [Eq. (23)], to minimize the cost using $\delta t = -\frac{B}{A}$ [Eqs. (29) and (30)].

4) Repeat steps 2 and 3 until $\delta t_{i+1} - \delta t_i < \epsilon$, where $\epsilon = 10^{-9}$ for our simulations.

Results

The algorithm described previously is designed to correct the position and velocity of a spacecraft after it has drifted away from its nominal trajectory due to an initial error. The question is, for how long after the initial error is it possible to correct the position? After a certain amount of time, the correction algorithm will not converge to a transfer orbit with maneuvers that have acceptable costs. The longer a spacecraft follows an erroneous trajectory, the more difficult it is to correct. Therefore, after a certain point, as long as the spacecraft follows the correct manifold path, it makes more sense to reset the orbit once it reaches the unstable manifold instead of using the technique described in this section.

The first set of examples presented have initial errors that follow the realistic model of gravity field uncertainty described in [8]. For each long lifetime orbit case, random initial position errors in the radial, cross-track, and along-track directions are introduced, and the trajectory is integrated for 1, 5, 10, and 20 days before the correction is made. For each case, 40 simulations are performed, and the average cost for each maneuver is computed. Corrections are not made after periods of time longer than 20 days because after that length of time, the trajectory has drifted far enough away from the nominal trajectory such that this method is not feasible. This is likely because the method is based on an initial guess which is the ideal transfer occurring in the absence of all perturbations. It also assumes that the initial and final orbits are coplanar which is, in general, not the case. However, for corrections done within 20 days of the initial error, these assumptions are valid and the algorithm converges to a transfer orbit with low-cost maneuvers. After the trajectory has evolved for longer, the algorithm does not always converge to a transfer orbit, and when it does, the costs are sometimes very large. Therefore, this method is valid only when the spacecraft has not drifted too far from the nominal trajectory.

The resulting costs for the two maneuvers with the error model described above are shown in Table 6. The factors to be considered when determining when the correction should be made are how quickly after discovering that the trajectory is not on the nominal trajectory can the correction be performed, and when it is most cost effective to perform the correction. In examining Table 6, we see that the lowest cost correction occurs at the 1 day mark. However, depending on when it becomes known that the spacecraft is not on the nominal trajectory, it might not be possible to perform the maneuver after 1 day. Therefore, the fact that the cost is still relatively low for corrections after 5 and 10 days is a useful result showing that it is not necessary to perform the correction very close to the time when the error is discovered. These results show that performing a correction maneuver within about a week or two from the time of the initial error is feasible.

The distributions used to compute initial errors for the results in Table 6 are those designated in [8] as the most likely orbit uncertainty values for the science portion of a mission to Europa. As previously noted, these orbit uncertainty values were obtained by assuming that before the science phase of the mission, the gravity field of Europa could be determined more accurately than the currently available values. Therefore, it is important to study the effect of larger levels of orbit uncertainty on the ability to make corrections to the spacecraft's position. Table 7 shows results corresponding to initial error values double the size of those in Table 6. In other words, the standard deviations of the error distributions are 2 times the values in [8]. It is not surprising that an increase in the initial position error leads to a decrease in the length of time that can elapse for a correction to be possible. For the results in Table 7, attempts to do a correction after 20 days caused errors in the convergence of the transfer orbit, and large costs when a transfer orbit was found. Therefore, the results shown are for corrections after 1, 5, 10, and 15 days. First, note that the total cost to return the spacecraft to its nominal trajectory is larger in this case than for the results in Table 6. This is not surprising because the initial errors are larger in this case, and so larger maneuvers are needed. However, the costs for the corrections after 1,

Table 6 Average cost to correct a science orbit after an initial position error

Frozen orbit inclination	1 day $\Delta v_1 + \Delta v_2$ m/s	5 days $\Delta v_1 + \Delta v_2$ m/s	10 days $\Delta v_1 + \Delta v_2$ m/s	20 days $\Delta v_1 + \Delta v_2$ m/s
70 deg	0.0989	0.1441	0.3733	0.5449
85 deg	0.2190	0.3589	0.8830	2.3885
95 deg	0.1642	0.2986	0.6010	3.7737
105 deg	0.1547	0.2949	0.3299	1.8024

Table 7 Average cost to correct a science orbit after a larger initial position error

Frozen orbit inclination	1 day $\Delta v_1 + \Delta v_2$ m/s	5 days $\Delta v_1 + \Delta v_2$ m/s	10 days $\Delta v_1 + \Delta v_2$ m/s	15 days $\Delta v_1 + \Delta v_2$ m/s
70 deg	0.2256	0.2466	0.8433	0.7966
85 deg	0.3746	0.7773	1.4339	1.3294
95 deg	0.4414	0.6415	1.3459	2.4245
105 deg	0.2733	0.3783	0.7837	1.8184

5, and sometimes 10 days are still relatively low, and corrections are feasible once again even if it is necessary to wait for a few days after the initial error. The results for both error models are consistent because as time goes on, the deviation between the erroneous trajectory and the nominal trajectory gets larger, increasing the cost of the correction in the same way that a larger initial error also increases the cost of the correction.

Conclusions

We have described two different techniques that can be used to control a long lifetime science orbit and apply them to the control of a Europa orbiter. The first assumes that the trajectory has reached the unstable manifold of a frozen orbit after having begun on the stable manifold. The goal of this method is to restart another long lifetime science orbit with characteristics very similar to the original orbit. After the target is computed, the two maneuvers necessary for the transfer are optimized to determine the sequence with the smallest total cost. We have found that steady-state costs on the order of 30 cm/s/day, corresponding to two burns with costs on the order of 16 m/s each are necessary for this transfer.

The second method is the computation of a transfer sequence that returns the spacecraft to its nominal trajectory after an initial position error, applied once again to the Europa orbiter case. Monte Carlo analysis is used to examine the effect of initial position errors, and it is found that by initializing the trajectory slightly above the 1-DOF system manifold, it is more likely that the trajectory will remain on the correct path, even after an initial position error. Then, a scheme is developed to return the spacecraft to its nominal trajectory using a two-maneuver sequence. An optimization is also performed in this section, such that the lowest total cost is obtained. We find that the sooner the trajectory is corrected, the lower the cost will be. However, if it is not possible to do the correction immediately, waiting up to 10 or 15 days does not increase the total cost too much. The costs required to return the spacecraft to its nominal trajectory are on the order of 1 m/s.

Acknowledgment

Marci Paskowitz Possner acknowledges the support of the Francois-Xavier Bagnoud (FXB) Foundation.

References

[1] Broucke, R., "Long-Term Third-Body Effects via Double Averaging," *Journal of Guidance, Control, and Dynamics*, Vol. 26, No. 1, 2003, pp. 27–32.
doi:10.2514/2.5041

[2] Scheeres, D., Guman, M., and Villac, B., "Stability Analysis of Planetary Satellite Orbiters: Application to the Europa Orbiter," *Journal of Guidance, Control, and Dynamics*, Vol. 24, No. 4, 2001, pp. 778–787.
doi:10.2514/2.4778

[3] Lara, M., San-Juan, J., and Ferrer, S., "Secular Motion Around Tri-Axial, Sychronously Rotating Planetary Satellites: Application to Europa," *Chaos*, Vol. 15, No. 4, 2005, pp. 1–13.

[4] San-Juan, J., Lara, M., and Ferrer, S., "Phase Space Structure Around Oblate Planetary Satellites," *Journal of Guidance, Control, and Dynamics*, Vol. 29, No. 1, 2006, pp. 113–120.
doi:10.2514/1.13385

[5] Lara, M., and Russell, R., "Computation of a Science Orbit About Europa," *Journal of Guidance, Control, and Dynamics*, Vol. 30, No. 1, 2007, pp. 259–263.
doi:10.2514/1.22493

[6] Paskowitz, M., and Scheeres, D., "Design of Science Orbits About Planetary Satellites: Application to Europa," *Journal of Guidance, Control, and Dynamics*, Vol. 29, No. 5, 2006, pp. 1147–1158.
doi:10.2514/1.19464

[7] Paskowitz Possner, M., "Orbit Design and Control of Planetary Satellite Orbiters in the Hill 3-Body Problem," Ph.D Thesis, The University of Michigan, Ann Arbor, MI, 2007.

[8] Thompson, P., Nandi, S., and Wong, M., "Orbit Determination Studies for a Low-Altitude Europa Orbiter," American Astronautical Society Paper 06-192, 2006.

[9] Brouwer, D., and Clemence, G., *Methods of Celestial Mechanics*, Academic Press Inc., New York, 1961, pp. 290, 337.

[10] Montenbruck, O., and Gill, E., *Satellite Orbits: Models, Methods, and Applications. Germany*, Springer–Verlag, Berlin, 2001, pp. 30, 57.

[11] Chobotov, V. (ed.), *Orbital Mechanics*, 2nd ed., AIAA, Reston, VA, 1996, p. 201.

[12] Anderson, J., Schubert, G., Jacobson, R., Lau, E., Moore, W., and Sjogren, W., "Europa's Differentiated Internal Structure: Inferences from Four Galileo Encounters," *Science*, Vol. 281, No. 5385, 1998, pp. 2019–2022.
doi:10.1126/science.281.5385.2019

[13] Guman, M., Roth, D., and Williams, B., "Navigation Feasibility Studies for the Europa Orbiter Mission," *Astrodynamics 1999*, Vol. 103, Advances in the Astronautical Sciences, Univelt, San Diego, CA, 1999, pp. 161–174.